Polyhedron 102 (2015) 424–433

Contents lists available at ScienceDirect

Polyhedron

journal homepage: www.elsevier.com/locate/poly

Anagostic, mono- and hexahapta interactions in Tl(I) dithiocarbamates: A new precursor for the preparation of Tl_2S nanoparticles

Govindaraju Gomathi [a], Subbiah Thirumaran [a,*], Samuele Ciattini [b]

[a] Department of Chemistry, Annamalai University, Annamalainagar 608 002, India
[b] Centro di Cristallografia Strutturale, Polo Scientifio di Sesto Fiorentino, Via della Lastruccia No. 3, 50019 Sesto Fiorentino, Firenze, Italy

ARTICLE INFO

Article history:
Received 5 July 2015
Accepted 30 September 2015
Available online 22 October 2015

Keywords:
Thallium(I) dithiocarbamates
X-ray structure
Anagostic interaction
Tl_2S nanoparticles
Powder X-ray diffraction

ABSTRACT

Two new homoleptic complexes, $[Tl(bzfdtc)]_2$ (**1**) and $[Tl(bu_{2\text{-}OH}bzdtc)]_2$ (**2**) (where bzfdtc = N-benzyl-N-furfuryldithiocarbamate and $bu_{2\text{-}OH}$bzdtc = (N-butyl-N-(2-hydroxybenzyl)dithiocarbamate), have been prepared and characterized by IR, NMR (^1H and ^{13}C), UV–Vis spectroscopy, cyclic voltammetry and single crystal X-ray structural analysis. X-ray crystallography revealed that both complexes are dimers. Both complexes show two monohapta Tl···C(S_2) interactions. The Tl···Tl distances are 3.635 and 3.719 Å for **1** and **2**, respectively. The phenyl ring of the bzfdtc ligand is coordinated (by a η^6 interaction) to the Tl^+ ion in complex **1**. A rare intramolecular anagostic C–H···Tl interaction is observed in complex **2**. Thallium sulfide nanoparticle samples **3** and **4** have been prepared from complex **1** using conventional heating and microwave irradiation, respectively. Samples **3** and **4** have been characterized by PXRD, EDAX, HR-TEM, UV–Vis absorption and fluorescence spectroscopy. PXRD measurements revealed rhombohedral and hexagonal phases for samples **3** and **4**, respectively. EDAX confirmed the formation of Tl_2S. HR-TEM images showed that the size and morphology of the Tl_2S nanoparticles are affected by the method of preparation (conventional heating compared to microwave irradiation).

1. Introduction

Dithisiderable interest in coordination chemistry [1]. Dithiocarbamates are highly versatile ligands that interact with main group metals and stabilize a variety of oxidation states in different coordination geometries [2,3]. The coordination numbers and geometries can be influenced by the relativistic effect of stereochemically active $6s^2$ lone pair of electrons on metal centres [1,4–7]. Thallium as a heavy element of group 13 has stable oxidation states of +1 and +3 [8]. Limited studies on thallium(I) dithiocarbamate complexes have been reported so far [4,5,9–21] because of the complexity of thallium(I) dithiocarbamate complexes which contain dimeric molecules of the same type but with different arrangements of the dimers. The linkages of the dimers lead to polymeric structures. These linkages are strongly influenced by the size and nature of the N-bound organic moiety of dithiocarbamate ligands [22].

The physical and chemical properties of materials deviate from those of the bulk on the reduction of size to the nanometer scale. Among the different classes of materials, nanostructural semiconductors have been extensively studied due to their potential applications and novel properties [23]. The thallium sulfide system is highly interesting because of the number of phases that it contains, including Tl_2S, Tl_4S_3, TlS, TlS_2, Tl_2S_3 and Tl_2S_9. Here, TlS and Tl_4S_3 are the double sulfides: $Tl^I[Tl^{III}S_2]$ and $Tl^I_3[Tl^{III}S_3]$, respectively, whereas TlS_2, Tl_2S_5 and Tl_2S_9 may be considered as poly sulfides, TlxSSn [24]. Thallium is an important ingredient in high temperature oxide superconductors [25,26]. Thallium compounds are useful in the production of optical glass, lenses for IR equipment and scintillation sensors [27]. Thallium monosulfide is an incongruent compound and it is used as a semiconductor [28,29]. Thallium chalcogenide coated polymers find use in photonic applications [30,31]. Metal dithiocarbamate complexes have been used as single source precursors for the preparation metal sulfide nanoparticles [32]. The phase and morphology of the metal sulfides are often influenced by the precursor as well as by the solvent and thermolysis temperature [33]. In this paper we report the synthesis, spectroscopic and single crystal X-ray structures of $[Tl(bzfdtc)]_2$ (**1**) and $[Tl(bu_{2\text{-}OH}bzdtc)]_2$ (**2**) (where bzfdtc = N-benzyl-N-furfuryldithiocarbamate and $bu_{2\text{-}OH}$-bzdtc = (N-butyl-N-(2-hydroxybenzyl)dithiocarbamate). The preparation of Tl_2S nanoparticles from complex **1** using conventional heating and microwave irradiation methods and their characterization by PXRD, HR-TEM, EDS analysis, UV–Vis absorption and fluorescence spectroscopy are also presented.

* Corresponding author at: Department of Chemistry, Annamalai University, Annamalainagar 608 002, Tamil Nadu, India. Tel.: +91 9842897597.
E-mail address: sthirumaran@yahoo.com (S. Thirumaran).

http://dx.doi.org/10.1016/j.poly.2015.09.071
0277-5387/

2. Experimental

All reagents and solvents were commercially available high grade materials [Merck/Sd fine/Himedia] and used as received. Elemental analysis was performed using a Perkin Elmer 2400 series II CHN analyzer. IR spectra were recorded on a thermo NICOLET AVATAR 330 FT-IR spectrophotometer for complex **1** and a THERMO SCIENTIFIC NICOLET iS_5 IR spectrometer for complex **2**. The $^1H/^{13}C$ NMR spectra were recorded on a BRUKER 400/100 MHz NMR spectrometer at room temperature in $CDCl_3$ solvent. The powder X-ray diffraction (XRD) patterns of the Tl_2S nanoparticles were recorded at room temperature using a Bruker D8 Advance X-ray diffraction system with Mo Kα radiation. High resolution–transmission electron microscopy (HR-TEM) was performed with a JEOL 3010, 300kv instrument equipped with a UHR polepiece. Energy dispersive X-ray analysis (EDS) was carried out with an Oxford EDAX housed in the TEM. UV–Vis absorption spectra were measured on a Shimadzu UV-1650 PC double beam UV–Visible spectrophotometer with the samples dispersed in ethanol at room temperature. Fluorescence spectra were recorded using a Perkin Elmer 1555 fluorescence spectrophotometer at room temperature.

2.1. X-ray crystallography

Diffraction data for **1** and **2** were recorded on Bruker axis Kappa apex II and Xcalibur, Sapphire 3 diffractometers, using graphite-monochromated Mo Kα radiation (λ = 0.71073 Å) at an ambient temperature. The structures were solved by SIR 92 [34] and refined by full-matrix least square methods in SHELXL-97 [35]. All non-hydrogen atoms were refined anistrophically and the hydrogen atoms were refined isotropically. Details of the crystal data and structure refinement parameters for **1** and **2** are summarized in Table 1. Selected bond lengths and angles for **1** and **2** are given in Table 2.

2.2. Preparation of the amines

N-benzyl-N-furfurylamine and N-butyl-N-(2-hydroxybenzyl) amine were prepared by general methods, as reported earlier [36].

Table 2
Selected bond lengths (Å) and bond angles (°) for complexes **1** and **2**.

1		**2**	
Tl1–S2^i	3.055(3)	Tl1–S2	3.0205(13)
Tl1–S1	3.082(3)	Tl1–S2^i	3.0647(13)
Tl1–S2	3.062(3)	Tl1–S1	3.0909(14)
Tl1–S1^i	3.114(3)	Tl1–S1^i	3.1492(15)
Tl1–Tl1^i	3.6451(8)	Tl1–Tl1^i	3.7195(4)
S1–C1	1.728(10)	S1–C1	1.713(5)
S2–C1	1.711(11)	S2–C1	1.738(5)
N1–C1	1.347(15)	S2–Tl1–S2^i	104.64(3)
S2–Tl1–S1	57.90(7)	S2–Tl1–S1	57.82(3)
S2–Tl1–S2^i	107.12(7)	S2–Tl1^i–S1^i	79.28(3)
S1^i–Tl–S2^i	80.97(8)	S2–Tl1–S1^i	79.03(3)
S2^i–Tl1^i–S1^i	57.64(7)	S2^i–Tl1–S1^i	56.77(3)
S1–Tl1–S1^i	107.67(7)	S1–Tl1–S1^i	106.83(3)
S2–Tl1–S1^i	79.72(8)	S2–Tl1–Tl1^i	52.86(2)
S2–Tl1–Tl1^i	53.22(6)	S2–Tl1^i–Tl1	51.78(2)
S1–Tl1–Tl1	54.49(6)	S1–Tl1–Tl1^i	54.14(3)
S2^i–Tl1–Tl1^i	53.91(6)	S1–Tl1–Tl1^i	52.69(3)
S1^i–Tl1–Tl1^i	53.17(5)	C1–S1–Tl1	84.66(16)
C1–S1–Tl1	84.8(4)	C1–S1–Tl1^i	83.91(16)
C1–S1–Tl1^i	83.5(4)	Tl1–S1–Tl1^i	73.17(3)
Tl1–S1–Tl1^i	72.88(6)	C1^i–S2^i–Tl1	86.48(16)
C1–S2–Tl1^i	85.6(4)	C1–S2–Tl1^i	86.20(15)
Tl1–S2–Tl1^i	72.33(7)	Tl1–S2^i–Tl1^i	75.35(3)
N1–C1–S1	119.9(8)		
N1–C1–S2	120.4(7)		
S1–C1–S2	119.8(7)		

For complex **1**, symmetry: $i = 1 - x,\ 2 - y,\ 2 - z$; for complex **2**, symmetry: $i = 1.5 - x,\ ½ + y,\ z$.

2.3. Preparation of complex 1

N-benzyl-N-furfurylamine (0.75 g, 4 mmol) and carbon disulfide (0.3 mL, 4 mmol) were dissolved in ethanol (20 mL) and stirred for 30 min at 5 °C. Thallium(I) chloride (0.8 g, 4 mmol) was dissolved in 30 mL of hot water and added to the solution. A pale yellow powder precipitated, which was filtered and dried (Scheme 1).

Yield: 73%. Mp: 120 °C. IR (KBr, cm^{-1}): 1447 (ν_{C-N}), 979 (ν_{C-S}). ^1H NMR (400 MHz, $CDCl_3$) δ, ppm: 5.37 (s,–C$\underline{H}_2$-(furyl)); 5.20 (s, –C$\underline{H}_2$–(benzyl)); 6.36–7.38 (aromatic protons). ^{13}C NMR

Table 1
Crystal data, data collection and refinement parameters for **1** and **2**.

	1	**2**
Empirical formula	$C_{13}H_{12}NOS_2Tl$	$C_{12}H_{16}NOS_2Tl$
FW	466.73	458.75
Crystal dimensions/mm	0.43 × 0.21 × 0.13	0.3 × 0.2 × 0.1
Crystal system	monoclinic	orthorhombic
Space group	$P2_1/c$	$Pbca$
a (Å)	10.2363(2)	11.0950(4)
b (Å)	8.81170(10)	9.3810(2)
c (Å)	16.0169(3)	27.5690(8)
α (°)	90	90.00
β (°)	101.405(2)	90.00
γ (°)	90	90.00
V (Å^3)	1416.1(4)	2869.44(15)
Z	4	8
D_{calc} (g cm^{-3})	2.189	2.124
μ (cm^{-1})	24.571	11.532
$F(000)$	872	1728
λ (Å)	CuK_α′ 1.54184	MoK_α 0.71073
θ range (°)	4.41-72.34	4.10-32.41
Index ranges	$-12 \leqslant h \leqslant 12,\ 10 \leqslant k \leqslant 10,\ -19 \leqslant l \leqslant 17$	$-16 \leqslant h \leqslant 15,\ -13 \leqslant k \leqslant 13,\ -39 \leqslant l \leqslant 36$
Reflections collected	13061	14525
Observed reflections [$I > 2\sigma\ (I)$]	2283	3568
Weighting scheme	Calc. $W = 1/(\sigma^2(F_o^2) + (0.1220p)^2 + 1.2067p)$ where $p = (F_o^2 + 2F_c^2)/3$	Calc. $W = 1/(\sigma^2(F_o^2) + (0.0247p)^2 + 9.0917p)$ where $p = (F_o^2 + 2F_c^2)/3$
Number of parameters refined	163	158
$R[F^2 > 2\sigma\ (F^2)]$, $wR(F^2)$	0.0679, 0.1652	0.0760, 0.0850
Goodness-of-fit (GOF)	1.147	1.034

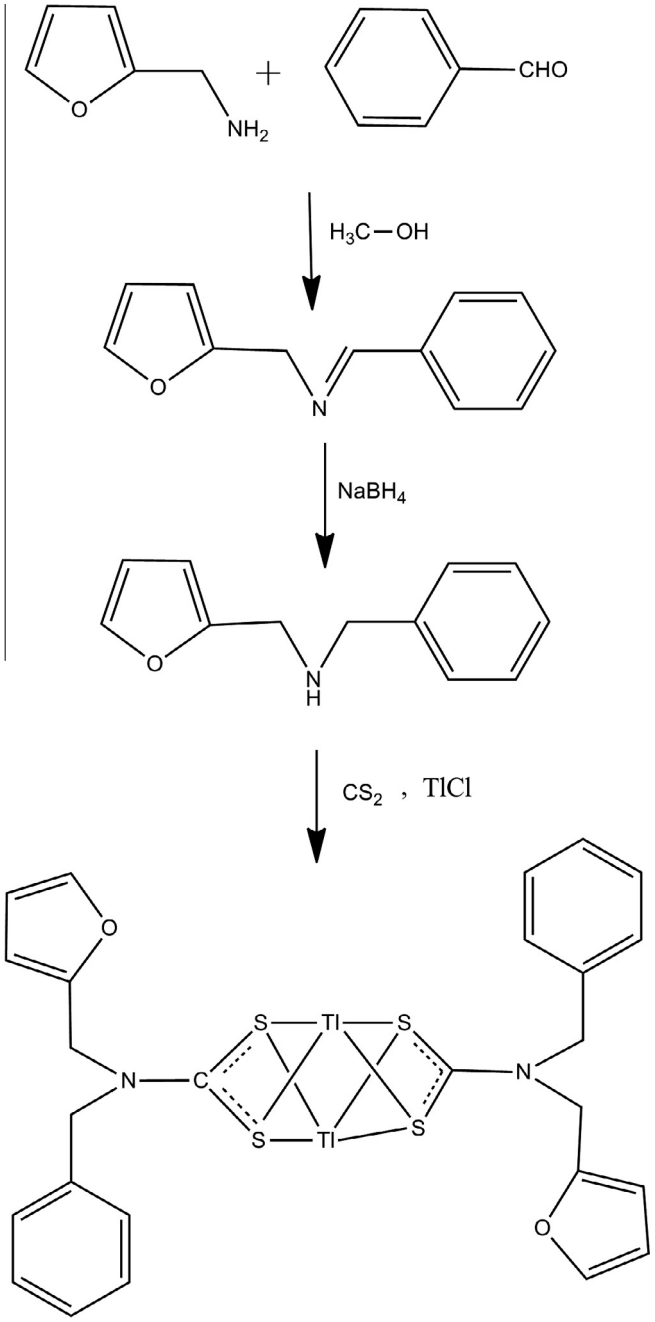

Scheme 1. Preparation of complex **1**.

(100 MHz, $CDCl_3$) δ, ppm: 47.7 (–$\underline{C}H_2$–(benzyl)); 55.2 (–$\underline{C}H_2$–(furyl)); 109.7, 110.5, 142.4, 150.1 (furyl ring carbons); 127.7–136.3 (aromatic ring carbons). *Anal.* Calc. for $C_{26}H_{24}S_4N_2O_2Tl_2$: C, 43.03; H, 3.33; N, 3.86. Found: C, 42.81; H, 3.27; N. 3.78%.

2.4. Preparation of complex 2

A method similar to that described for the synthesis of **1** was adopted, however N-butyl-N-(2-hydroxybenzyl)amine was used instead of N-benzyl-N-furfurylamine (Scheme 2).

Yield: 71%. Mp: 90 °C. IR (KBr, cm^{-1}): 1457 (ν_{C-N}), 1036 (ν_{C-S}), 3444 (ν_{OH}). ^1H NMR (400 MHz, $CDCl_3$) δ, ppm: 0.94 (m, N–CH_2–CH_2–CH_2–$C\underline{H}_3$); 1.33 (dd, N–CH_2–CH_2–$C\underline{H}_2$–CH_3); 1.67 (dd, N–CH_2–$C\underline{H}_2$–CH_2–CH_3); 3.89 (m, N–$C\underline{H}_2$–CH_2–CH_2–CH_3); 4.52 (s, 2OH–C_6H_4–$C\underline{H}_2$–N); 5.29 (s, 2OH–C_6H_4–CH_2–N); 6.88–7.23 (aromatic protons). ^{13}C NMR (100 MHz, $CDCl_3$) δ, ppm: 13.9 (N–CH_2–CH_2–CH_2–$\underline{C}H_3$); 20.0 (N–CH_2–CH_2–$\underline{C}H_2$–CH_3); 28.6 (N–CH_2–$\underline{C}H_2$–CH_2–CH_3); 51.6 (N–$\underline{C}H_2$–CH_2–CH_2–CH_3); 53.4 (2OH–C_6H_4–$\underline{C}H_2$–N); 117.1–131.8 (aromatic carbons); 155.7 (ipso carbons); 202.6 (N$\underline{C}S_2$). *Anal.* Calc. for $C_{24}H_{32}S_4N_2O_2Tl_2$: C, 31.41; H, 3.51; N, 3.05. Found: C, 30.8; H, 3.40; N, 2.97%.

2.5. Preparation of thallium sulfide (Tl_2S) (sample 3)

0.5 g of $[Tl(bzfdtc)]_2$ was dissolved in 15 ml ethylenediamine in a round bottom flask and then the contents of the flask were refluxed for 1 h. The black precipitate obtained was filtered off and washed with methanol.

2.6. Preparation of thallium sulfide (Tl_2S) (sample 4)

0.5 g of $[Tl(bzfdtc)]_2$ was dissolved in 15 ml ethylenediamine in a 100 ml beaker and then the reaction was carried out by microwave irradiation for 2 min. The black precipitate obtained was filtered off and washed with methanol.

3. Results and discussion

3.1. Infrared spectral studies

Infrared spectra of complexes **1** and **2** are shown in Figs. S1 and S2. In the IR spectra of the complexes, a strong band observed at 1447 and 1457 cm^{-1} for **1** and **2**, respectively, is assigned to the N–CS_2 stretching mode [37]. This indicates that the C–N bond order is intermediate between a single and a double bond [38], suggesting strong electron delocalization in the dithiocarbamate moiety. A band with medium intensity due to the stretching mode of the C–S bond appeared at 979 and 1036 cm^{-1} for **1** and **2**, respectively [39]. In the IR spectrum of **2**, a broad band observed at 3444 cm^{-1} is characteristic of the ν_{OH} vibration.

3.2. NMR spectral studies

NMR spectra were recorded at room temperature using TMS as an internal reference. $CDCl_3$ was used as the solvent. The ^{13}C NMR spectra were recorded in the proton decoupled mode. The structures of the ligands are shown in Schemes 1 and 2. The ^1H and ^{13}C NMR spectra of complexes **1** and **2** are given in Figs. S3–S6.

3.2.1. ^1H NMR spectral studies

The ^1H NMR spectrum of **1** shows two singlets at δ 5.20 and 5.37 ppm due to the methylene protons of the benzyl and furyl groups. A triplet at δ 2.68 ppm and a singlet at δ 5.29 ppm observed in **2** are assigned to the methylene protons adjacent to the nitrogen atom. These methylene protons are affected by the complexation to a maximum extent as a result of deshielding. In complex **2** the other methylene and methyl protons appear in the upfield region at δ 0.91–1.33 ppm. The hydroxy proton resonates at δ 5.29 ppm. The signals in the downfield region δ 6.88–7.23 ppm are due to the aromatic protons.

3.2.2. ^{13}C NMR spectral studies

In complex **1**, two signals observed in the aliphatic region (δ 47.7 and 55.2 ppm) are due to the furfuryl and benzyl methylene

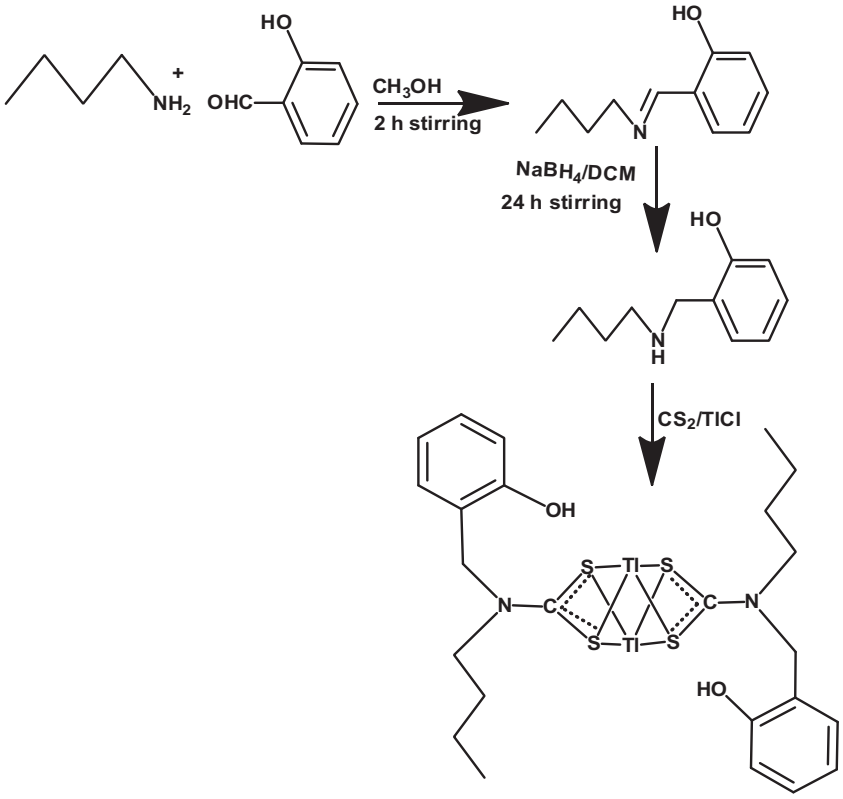

Scheme 2. Preparation of complex **2**.

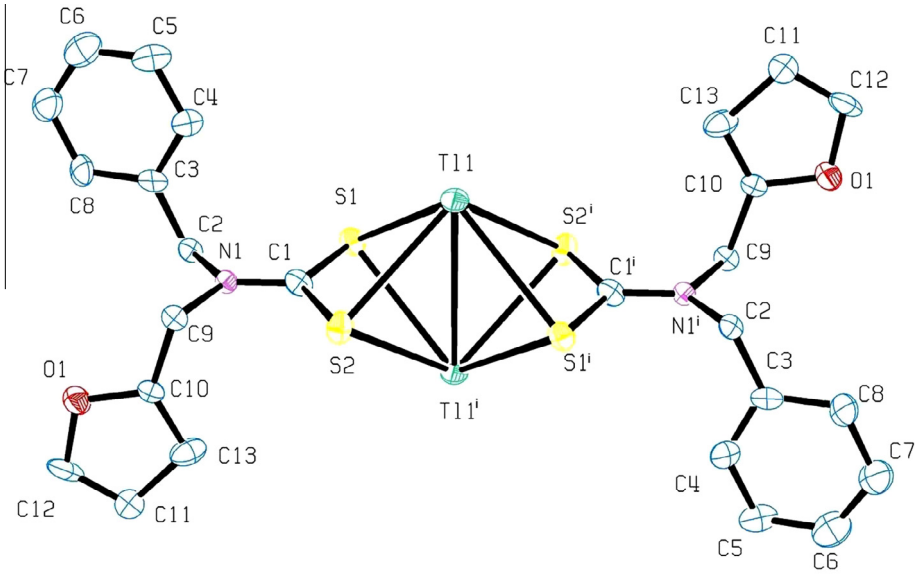

Fig. 1. ORTEP of complex **1**.

carbons. The proton and carbon chemical shift values of the furfuryl methylene group are lower than those of the benzyl methylene group. This is due to the delocalization of lone pair electrons of the oxygen atom within the furyl ring which increases the electron density on methylene unit of the furfuryl group [39]. In complex **2**, two signals at δ 51.6 and 53.40 ppm are due to the methylene carbon atoms of the butyl and hydroxybenzyl groups. A weak signal observed at δ 155.7 ppm is assigned to the *ipso* carbon atom. The NCS_2 carbon signals of **1** and **2** appeared at δ 206.7 and 202.6 ppm, respectively, indicating partial double bond character of the N–C bond in the dithiocarbamate ligand.

3.3. Electronic spectral studies

Electronic spectra of complexes **1** and **2** are given in Fig. S7. Complex **1** is pale yellow and **2** is colourless. Three bands observed

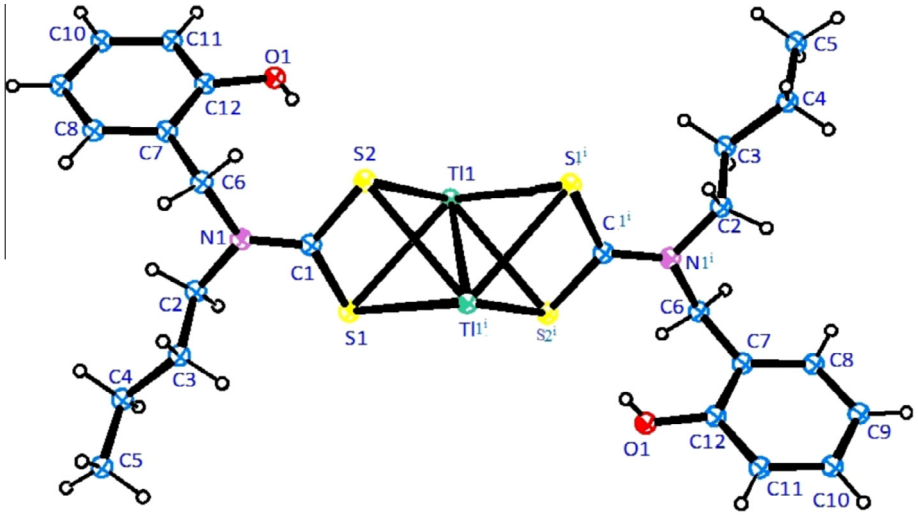

Fig. 2. ORTEP of complex **2**.

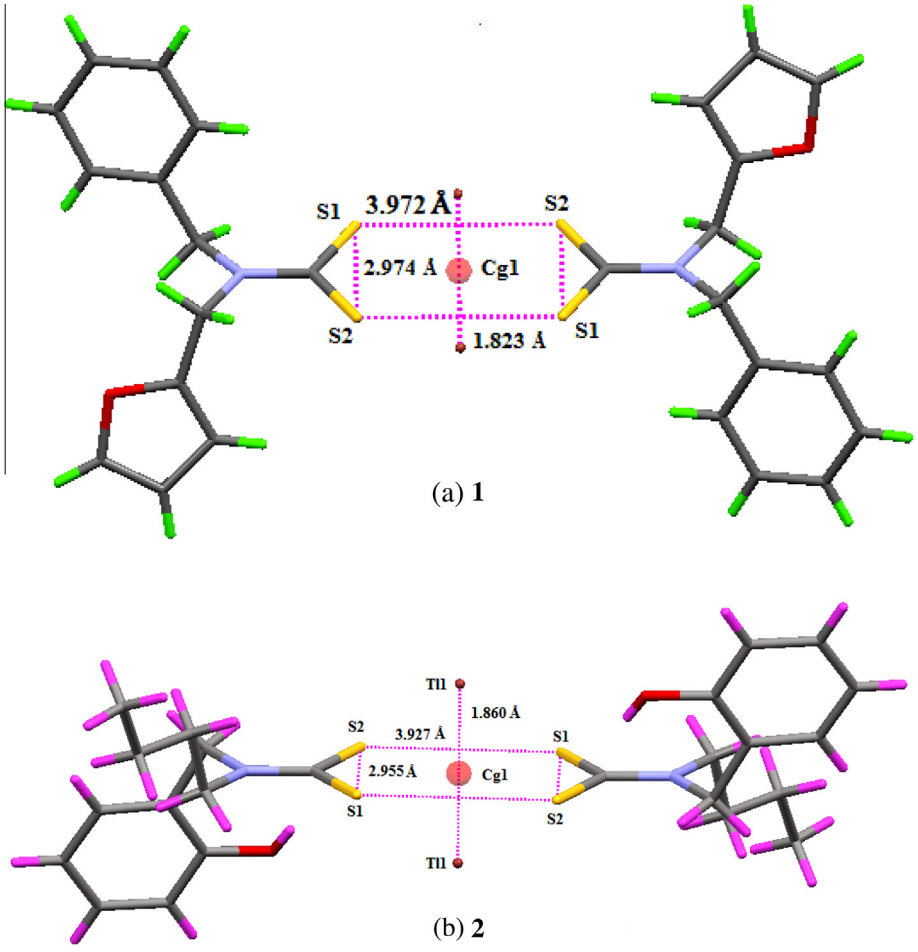

Fig. 3. View of the sulfur parallelogram (a) **1** and (b) **2**.

around 315, 270 and 236 nm for both the complexes are due to intraligand $\pi \rightarrow \pi^*$ transitions, mainly associated with N–C═S and S–C═S groups and an $n \rightarrow \pi^*$ transition located on the sulfur atoms (Figs. S7(a) and (b)). There are no d–d transitions as Tl(I) has a $6s^2 6p^1$ configuration [40].

3.4. Cyclic voltammetric studies

The cyclic voltammograms of **1** and **2** are shown in Fig. S8. The reduction potentials for complexes **1** and **2** are observed at −0.9152 and −0.6019 V, respectively. The reductions are

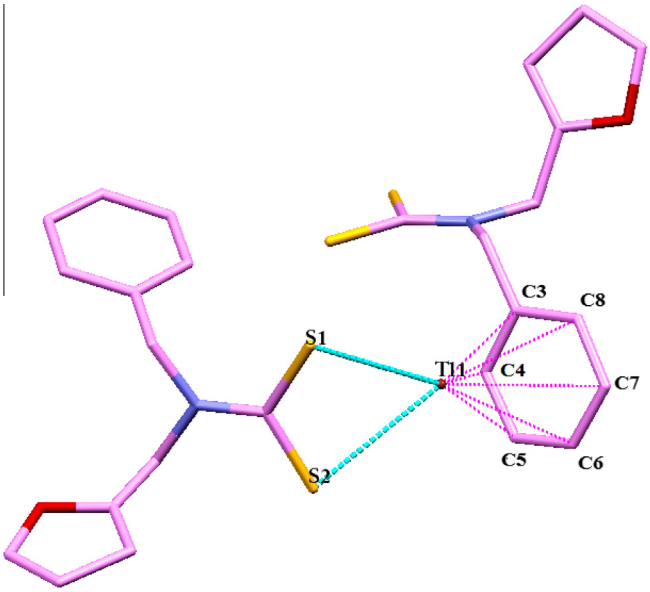

Fig. 4. Tl^{+}-arene interaction in complex **1**.

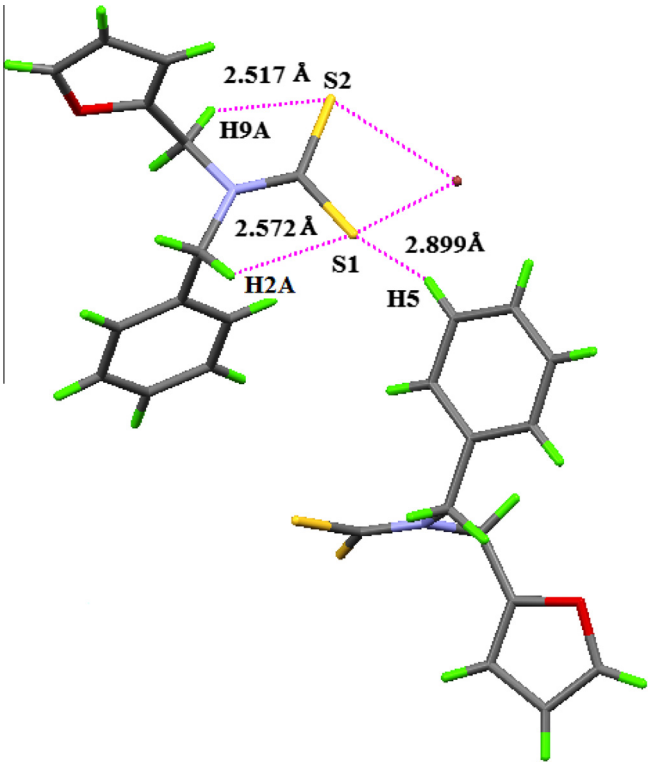

Fig. 5. Intramolecular and intermolecular C–H···S interactions in **1**.

irreversible and one electron processes. A one electron reduction process with the formation of Tl has been already proposed [66]: $Tl^{+} + e^{-} \rightarrow Tl$. This indicates that the oxidation state of thallium in both the complexes is +1.

3.5. Single crystal X-ray structural analysis of complexes 1 and 2

ORTEP diagrams of complexes **1** and **2** are shown in Figs. 1 and 2, respectively. In the asymmetric unit, the thallium center is bonded to the two sulfur atoms of the dithiocarbamate ligand at distances of Tl1-S1 = 3.062(3) and Tl1-S2 = 3.082(3) Å in complex **1** and Tl1-S1 = 3.0909(14) and Tl1-S2 = 3.0205(13) Å in complex **2**. Each thallium center in the asymmetric unit is bonded with two sulfur atoms of another centrosymmetrically related dithiocarbamate ligand at distances of 3.114 (3) and 3.055 (3) Å in complex **1**, and 3.0647(13) and 3.1492(14) Å in complex **2**, leading to a dimer. In addition, two monohapto interactions involving thallium and the C atom of the CS_2 moiety are observed to occur at distances of Tl···C1S_2 = 3.376 and Tl···C1$^{i}S_2$ = 3.386 Å for **1**, and Tl···C1S_2 = 3.422 and Tl···C1$^{i}S_2$ = 3.391 Å for **2**, with the carbon atom of dithiocarbamate ligands of an asymmetric unit and centro symmetrically related unit, respectively. In the dimeric unit, the thallium atoms are situated on either side of a sulfur parallelogram (Fig. 3) with edges of ~2.9 and ~3.9 Å, forming a bicapped parallelogram. In the dimer, the Tl···Tl distances for **1** and **2** are 3.6451(8) and 3.7195(4) Å, respectively, which are shorter than the sum of the van der Waals radii (3.92 Å), exhibiting the presence of a Tl···Tl interaction.

In the case of complex **1**, each thallium atom in the binuclear molecule is bonded to four sulfur atoms and there is a cation–π interaction (the arene π-system counts as a single donor), thus forming a distorted square pyramid. The centroid of the aryl ring (C3–C8) is situated 3.237 Å from the Tl^{+} ion. Since C_{arene}–Tl distances vary only slightly within a narrow range from 3.462 to 3.571 Å, the Tl^{+}–arene interaction can be regarded as true η^{6}–coordination, Fig. 4. Two intramolecular C–H···S (C9–H9···S2 = 2.517 (11) Å) and C2–H2···S1 = 2.572(11) Å) interactions take place between methylene hydrogen atoms (of benzyl and furfuryl groups) and the thioureide sulfur atom. This complex also displays a weak intermolecular C–H···S interaction (Fig. 5, Table 3).

In complex **2**, a C–H···Tl interaction is observed (Fig. 6). Generally, three types of C–H···M interactions are found, i.e. (i) hydrogen ion (ii) agostic and (iii) anagostic interactions [41–61]. Hydrogen bonds are 3-center-4-electron interactions within an almost linear geometry. Agostic interactions are usually referred to as 3-centered-2-electron interactions and characterized by M···H distances of ~1.8–2.2 Å and C–H···M bond angles of ~90–130°. Anagostic interactions are characterized by M···H distances of 2.3–2.9 Å and large M···H–C bond angles ~110–170°. Anagostic interactions are stabilized by d^{8} complexes. C–H···Tl interactions are rare [62–65]. In the present study, an intermolecular C–H···Tl (H···Tl = 3.198 Å and ∠C–H···Tl = 131.91°) is observed in complex **2**. The H···Tl distance is larger than the values found in complexes of d^{8} metal ions (M···H ~2.3–2.9 Å) [66]. This is due to the larger size of the Tl^{+} ion. Further stabilization of the complex is provided by intramolecular C–H···S (H2A···S1 = 2.633(11) and H6A···S2 = 2.531(10) Å) interactions with the hydrogen atoms of the dithiocarbamate methylene group and O–H···S (H···S 2.467 (10) Å) interactions (Fig. 7, Table 3).

3.6. Characterization of thallium sulfide nanoparticles

Tl_2S synthesized from complex **1** using conventional heating and microwave irradiation methods are represented as samples **3** and **4**, respectively. The PXRD patterns for samples **3** and **4** are given in Fig. 8. In the case of sample **3**, the sharp diffraction peaks reveal that the obtained Tl_2S nanoparticles are well crystalline. The diffraction peaks located at 2θ = 29.3°, 32.9°, 39.1°, 44.6° and 54.4° can be indexed respectively as (033), (116), (306), (330) and (229) planes of the rhombohedral phase with lattice constants a = 12.2(7) and c = 18.17(6), which are in good agreement with the Joint Committee on Powder Diffraction Standards JCPDS file No 89-2013 [67]. The presence of (012), (113) and (122) planes in the diffraction patterns of sample **4** is characteristic of the hexagonal phase of Tl_2S. This is in good agreement with the JCPDS

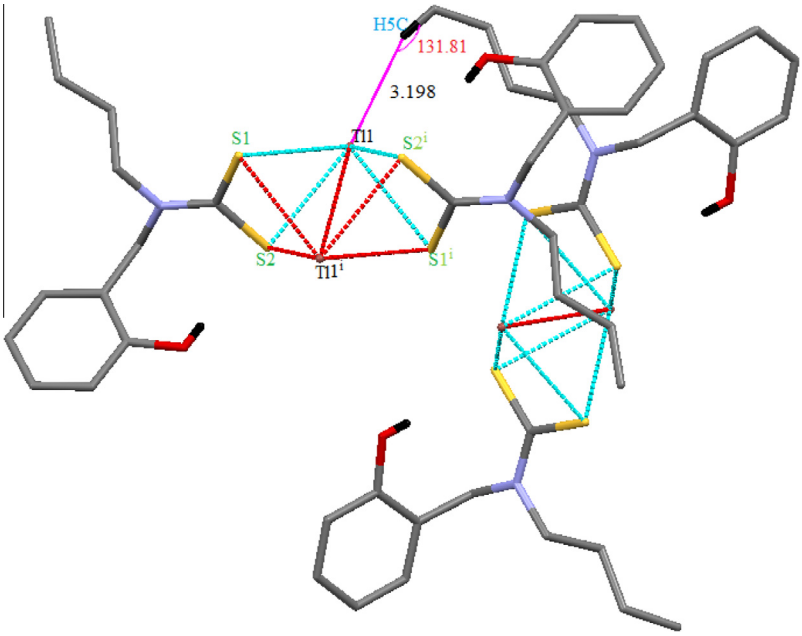

Fig. 6. Intermolecular anagostic interaction in complex **2**.

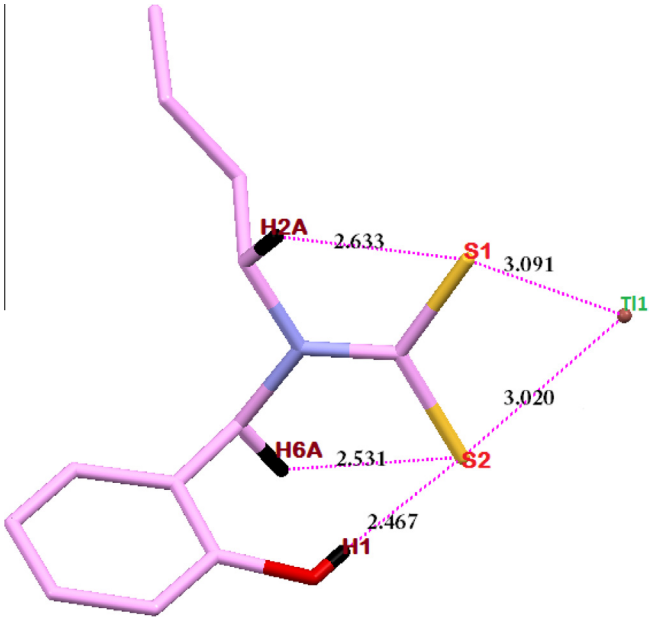

Fig. 7. Intramolecular S···H–C and S···H–O interactions in complex 2.

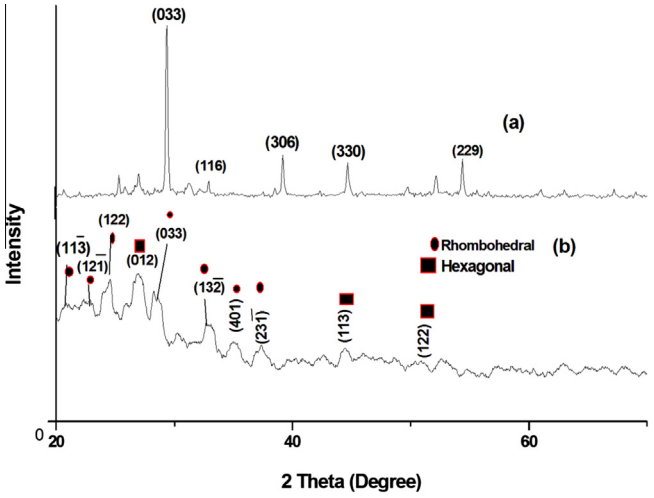

Fig. 8. Powder XRD patterns of Tl_2S (a) sample **3** and (b) sample **4**.

file No 44-0889 [68].The remaining diffraction peaks can also be assigned to the rhombohedral phase (JCPDS File no 89-2076) [67].

The energy dispersive X-ray spectra of **3** and **4** are shown in Figs. 9(a) and (b). The energy dispersive X-ray spectroscopic studies of samples **3** and **4** confirm that the elemental composition of samples **3** and **4** is Tl_2S.

HR-TEM images of samples **3** and **4** are shown in Figs. 10 and 11. The HR-TEM image of sample **3** shows that the particles are nanometric size and shapeless, in sample **4**, the particles are spherical in shape and the diameters of the particles are ~10 nm. The lattice plane spacing calculated from the HRTEM images (Figs. 10 and 11) are ca. 3.2 and 3.5 Å, corresponding to the (113) and (229) crystal planes of TlS samples **3** and **4**, respectively.

The UV–Vis absorption spectra of samples **3** and **4** in ethanol are shown in Fig. 12. The absorption maxima is observed at 273 nm for sample **3** and 293 nm for sample **4**. Both samples reveal a blue shift with respect to bulk Tl_2S, indicating a quantum confinement effect [69].

Fluorescence spectra of samples **3** and **4** are given in Fig. 13. The emission spectra were measured with a 270 nm excitation source. In the case of sample **3**, two broad emission peaks are observed at 362 and 419 nm. Only one broad emission peaks appeared at 362 nm for sample **4**. In both cases, the emission peak at 362 nm is due to the core state radioactive decay from the conduction band to the valence band. The additional emission at 419 nm in the fluorescence spectrum of sample **3** is attributed to the recombination of trapped electrons/holes in some surface defect states of the Tl_2S particles.

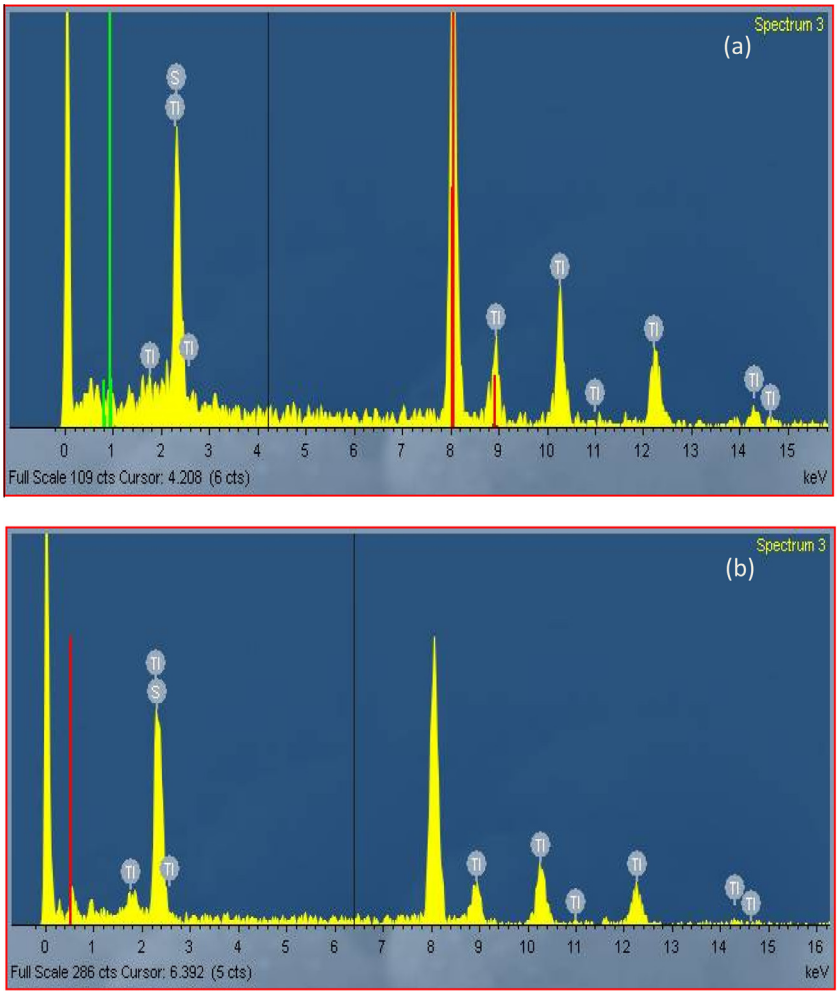

Fig. 9. EDAX spectra of (a) Tl_2S (sample **3**) and (b) Tl_2S (sample **4**).

Table 3
Geometric details of the hydrogen bonding (Å, °) for complexes **1** and **2** (D – donor; A – acceptor; H – hydrogen).

Interactions	D–H	H···A	D···A	D–H···A
*Complex **1***				
C(2)–H(2A)···S1	0.970	2.572(11)	3.069(12)	119.98
C(9)–H(9A)···S2	0.969	2.517(11)	2.997(11)	110.48
C(6)–H(6A)···S1	0.931	2.897(12)	3.063(11)	140.45
*Complex **2***				
C(2)–H(2A)···S1	0.970	2.633(11)	3.010(10)	103.43
C(6)–H(6A)···S2	0.970	2.531(10)	3.052(10)	113.65
O(1)–H(1)···S2	0.634	2.467(10)	3.101(11)	177.06

4. Conclusions

Complexes **1** and **2** have been prepared and characterized by elemental analyses, spectroscopic techniques and single crystal X-ray structural analysis. Interestingly, various interactions, namely η^1–Tl–C(S2), Tl···Tl, η^6–Tl···C phenyl ring, anagostic Tl···H–C, intramolecular C–H···S, intermolecular C–H···S and O–H···S interactions, are observed. These interactions depend on the size and electronic effects of the dithiocarbamate ligands and crystal packing effects. Tl_2S nanoparticles have been prepared from complex **1** using conventional heating and microwave irradiation methods. The microwave irradiation method yields spherical shape particles within 2 min. Shapeless particles are obtained after 1 h with the conventional heating method. Hence, the more suitable method for the preparation of Tl_2S nanoparticles is the microwave irradiation method.

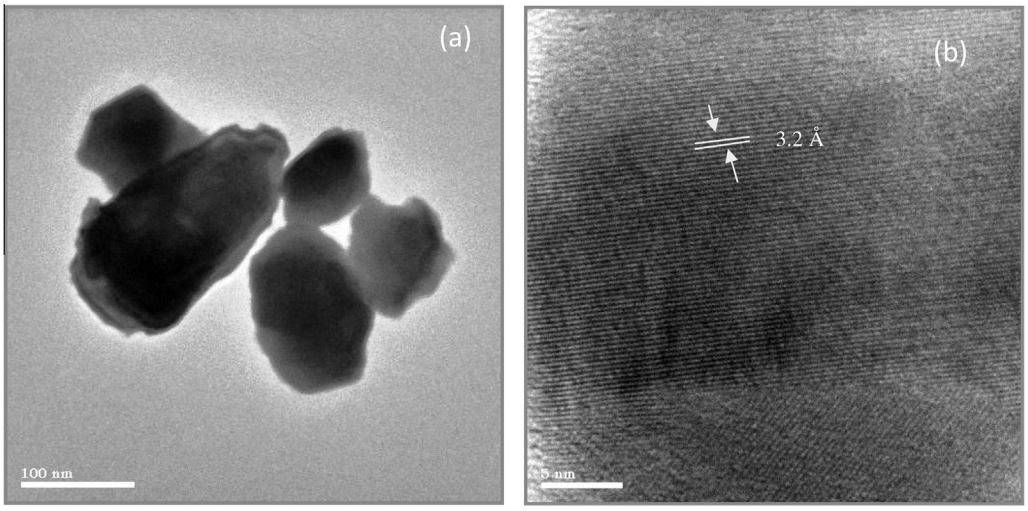

Fig. 10. HR-TEM image of Tl_2S (sample **3**).

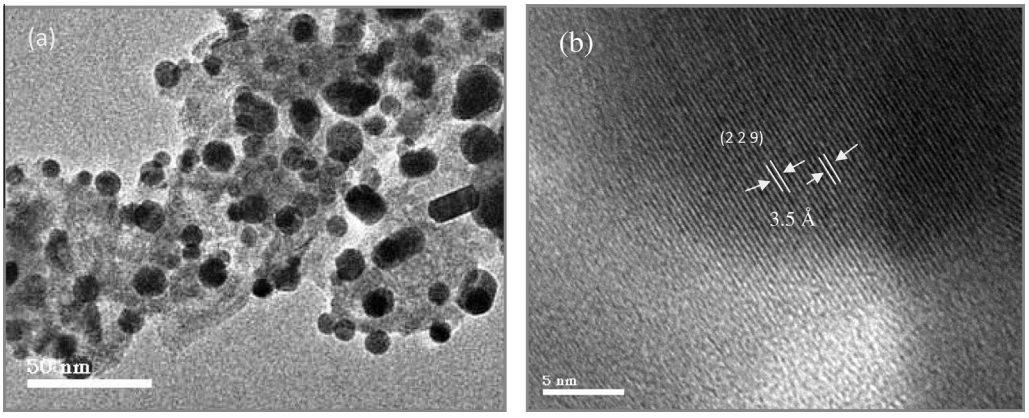

Fig. 11. HR-TEM image of Tl_2S sample **4**.

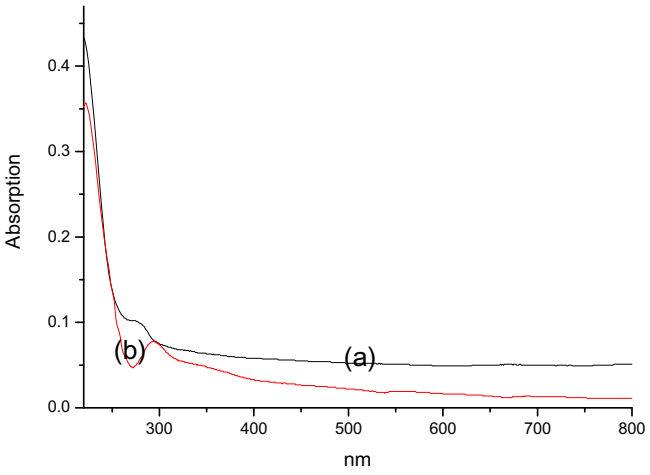

Fig. 12. UV–Vis spectra of Tl_2S (a) sample **3** and (b) sample **4**.

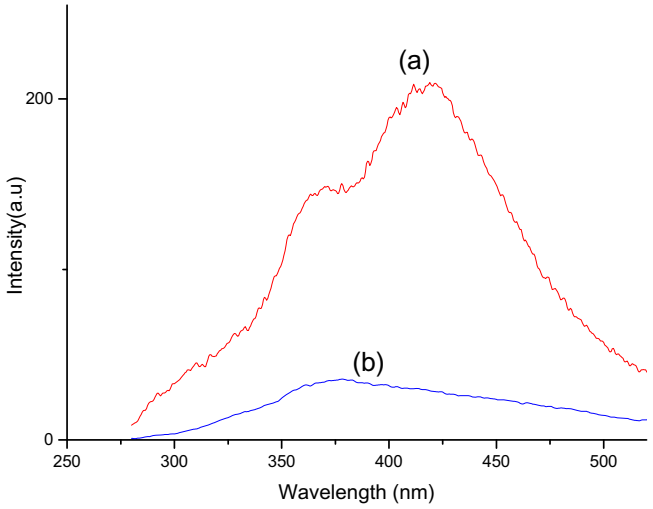

Fig. 13. Photoluminescence spectra of Tl_2S (a) sample **3** (b) sample **4**.

Appendix A. Supplementary data

CCDC 1427864 and 1057653 contain the supplementary crystallographic data for complexes **1** and **2**. These data can be obtained free of charge via http://www.ccdc.cam.ac.uk/conts/retrieving.html, or from the Cambridge Crystallographic Data Centre, 12 Union Road, Cambridge CB2 1EZ, UK; fax: (+44) 1223-336-033; or e-mail: deposit@ccdc.cam.ac.uk. Supplementary data associated with this article can be found, in the online version, at http://dx.doi.org/10.1016/j.poly.2015.09.071.

References

[1] L. Nilson, R. Hesse, Acta Chem. Scand. 23 (1969) 1951.
[2] R.P. Feazell, C.E. Carson, K.K. Klausmeyer, Inorg. Chem. 45 (2006) 935.
[3] P.J. Heard, K.D. Karlin, Prog. Inorg. Chem. 53 (2005) 1.
[4] E. Elfwing, H. Anacker-Eickhoff, R. Hesse, Acta Chem. Scand. 30 (1976) 335.
[5] N. Alexander, K. Ramalingam, C. Rizzoli, Inorg. Chim. Acta 365 (2011) 480.
[6] B. Krebs, A. Brommethaus, Angew. Chem. Int. Ed. Engl. 28 (1989) 1682.
[7] Y. Rong, J.H. Palmer, G. Parkin, Dalton Trans. 43 (2014) 1397.
[8] M. Sadegh, Y. Parasi, A. Morsali, Z. Anorg, Allg. Chem. 638 (2012) 451.
[9] A.V. Ivanov, O.A. Bredynk, A.V. Gerasimenko, O.N. Antzutkin, W. Forsling, Russ. J. Coord. Chem. 32 (2006) 339.
[10] H. Pritzkow, P. Jennische, Acta Chem. Scand. A29 (1975) 60.
[11] R.T. Griffin, K. Henrick, R.W. Matthews, M. McPartlin, J. Chem. Soc. Dalton Trans. (1980) 1550.
[12] S.-H. Hong, P. Jennische, Acta Chem. Scand. A32 (1978) 313.
[13] C. Burschka, Z. Anorg, Allg. Chem. 485 (1982) 217.
[14] H. Anacker-Eickhoff, P. Jennische, R. Hesse, Acta Chem. Scand. A29 (1975) 51.
[15] D.L. Kepert, C.L. Raston, N.K. Roberts, A.H. White, Aust. J. Chem. 31 (1978) 1927.
[16] P. Jennische, A. Olin, R. Hesse, Acta Chem. Scand. 26 (1972) 2799.
[17] P. Jennische, R. Hesse, Acta Chem. Scand. 27 (1973) 3531.
[18] H. Abrahamson, J.R. Heiman, L.H. Pignolet, Inorg. Chem. 14 (1975) 2070.
[19] J.S. Casas, M.V. Castano, C. Freire, A. Sanchez, J. Sordo, E.E. Castellano, J. Zukerman-Schpector, Inorg. Chim. Acta 216 (1994) 15.
[20] T.A. Rodina, A.V. Ivanov, O.A. Bredyuk, A.V. Gerasimenko, Koord. Khim. (Russ.) 35 (2009) 172.
[21] C. Rizzoli, K. Ramalingam, N. Alexander, Acta Crystallogr. E. 64 (2008) 1020.
[22] E. Elfwing, H. Anacker-Eickhoff, P. Jennische, R. Hesse, Acta Chem. Scand. A30 (1976) 335.
[23] J.M. Bruchee, M. Moronne, P. Gin, S. Weiss, A.P. Alivasators, Science 281 (1998) 2013.
[24] A.G. Lee, The chemistry of thallium, in: P.L. Robinson (Ed.), Monograph 14 in the Series Topics in Inorganic Chemistry, Elsevier, Amsterdam, 1971.
[25] S.C. Speller, Mater. Sci. Technol. 19 (2003) 269.
[26] G. William, A. Harter, M. Hermann, Z.Z. Sheng, Appl. Phys. Lett. 53 (1988) 1119.
[27] E.S. Ferreira, M. Mulato, Braz. J. Phys. 42 (2012) 186.
[28] V. Estrella, M.T.S. Nair, P.K. Nair, Thin Solid Films 414 (2002) 281.
[29] V.P. Aliev, Sh.G. Gasimov, T.G. Mammadov, T.S. Mammadov, A.I. Nadjafov, Mirhasan Yu. Seyidov, Phys. Solid State 48 (2006) 2322.
[30] V. Janickis, R. Stokiene, Chemija 21 (2010) 17.
[31] I.M.A. Shraf, H.E. Ish Ackh, A.M. Bodr, Cryst. Res. Technol. 39 (2004) 63.
[32] N.L. Pickette, P. O' Brien, Chem. Rec. 1 (2001) 467.
[33] D.O. Monterio, H.I.S. Nogueiva, T. Trindade, Chem. Mater. 13 (2001) 2103.
[34] A. Altomare, M.C. Burla, M. Camali, G. Cascarano, C. Giacovazzo, A. Guagliardi, G. Polidori, J. Appl. Crystallogr. 27 (1994) 435.
[35] G.M. Sheldrick, Acta Crystallogr. A 64 (2008) 112.
[36] H. Nabipour, S. Ghammany, S.A. Shwri, Z.S. Aghbolangh, J. Org. Chem. 2 (2010) 75.
[37] A.C. Costa Jr., G.F. Ondar, O. Versiane, J.M. Ramos, T.G. Santos, A.A. Martin, L. Raniero, G.G.A. Bussi, C.A. Téllez Soto, Spectrochim. Acta A 105 (2013) 251.
[38] L. Ronconi, L. Giovagnini, C. Marzano, F. Bettìo, R. Graziani, G. Pilloni, D. Fregona, Inorg. Chem. 44 (2005) 1867.
[39] G. Gomathi, S. Hussain Dar, S. Thirumaran, S. Ciattini, S. Selvanayagam, C. R. Chim. 18 (2015) 499.
[40] N. Manav, A.K. Mishra, N.K. Kaushik, Spectrochim. Acta A 65 (2006) 32.
[41] M. Brookhart, M.L.H. Green, G. Parkin, Proc. Natl. Acad. Sci. USA 104 (2007) 6908.
[42] C. Taubmann, K. Ofele, E. Herdweek, W.A. Herrmann, Organometallics 28 (2009) 4254.
[43] W. Yao, O. Eisenstein, R.H. Crabtree, Inorg. Chim. Acta 254 (1997) 105.
[44] J. Sabmannshausen, Dalton Trans. 41 (2012) 1919.
[45] K.A. Siddiqui, E.R.T. Tickink, Chem. Commun. 49 (2013) 8501.
[46] S. Scholer, M.H. Wahl, N.I.C. Wurster, A. Puls, C. Hattig, G. Dyker, Chem. Commun. 50 (2014) 5909.
[47] D. Brago, F. Grepioni, E. Tedesco, K. Biradha, G.R. Desiraju, Organometallics 16 (1997) 1846.
[48] A.G. Jarvis, P.E. Sehnal, S.E. Bajwa, A.C. Whitwood, X. Zhang, M.S. Cheung, Z. Lin, I.J.S. Fairlamb, Chem. Eur. J. 19 (2013) 6034.
[49] M. Baya, U. Belio, A. Martin, Inorg. Chem. 53 (2014) 189.
[50] F. Kraus, H. Schmidbaur, S.S. Al-juaid, Inorg. Chem. 52 (2013) 9669.
[51] S. Rizzato, J. Berges, S.A. Mason, A. Albinati, J. Kozelka, Angew. Chem. Int. Ed. 49 (2010) 7440.
[52] R. Angamuthu, L.L. Gelauff, M.A. Siegler, A.L. Spek, E. Bouwman, Chem. Commun. 19 (2009) 2700.
[53] B. Singh, M.G.B. Drew, G.K. Kohn, K.C. Molloy, N. Singh, Dalton Trans. 40 (2011) 623.
[54] G. Rajput, V. Singh, A.N. Gupta, M.K. Yadav, V. Kumar, S.K. Singh, A. Prashad, M. G.B. Drew, N. Singh, Cryst. Eng. Comm. 15 (2013) 4676.
[55] V. Singh, R. Chauhan, A.N. Gupta, V. Kumar, M.G.B. Drew, L. Bahadur, N. Singh, Dalton Trans. 43 (2014) 4752.
[56] A.N. Gupta, V. Kumar, V. Singh, K.K. Manar, M.G.B. Drew, N. Singh, Cryst. Eng. Comm. 16 (2014) 9299.
[57] H.V. Huynh, L.R. Wong, P.S. Ng, Organometallics 27 (2008) 2231.
[58] X. Ribas, C. Calle, A. Poater, A. Casitas, L. Gomez, R. Xifra, T. Parella, J. Benet-Buchholz, A. Schweiger, G. Mitrikas, M. Sola, A. Llobet, T.D.P. Stack, J. Am. Chem. Soc. 132 (2010) 12299.
[59] W.H. Bernskoetter, C.K. Schauer, K.I. Goldberg, M. Brookhart, Science 326 (2009) 553.
[60] M. Albreeht, G. Van Koten, Angew. Chem. Int. Ed. 40 (2001) 3738.
[61] M. Stepien, L. Latos-Grazynski, Acc. Chem. Res. 38 (2005) 88.
[62] C. Chen, R.F. Jordan, J. Organomet. Chem. 695 (2010) 2542.
[63] E. Craven, E. Muthu, D. Lundberg, S. Temizdemir, S. Deehert, H. Brombacher, C. Janiak, Polyhedron 21 (2002) 553.
[64] T. Fillebeen, T. Hascall, G. Parkin, Inorg. Chem. 36 (1997) 3787.
[65] V. Kumar, V. Singh, A.N. Gupta, M.G.B. Drew, N. Singh, Dalton Trans. 44 (2014) 1716.
[66] K. Ramalingam, C. Rizzoli, N. Alexander, Springer–Verlag Wein 144 (2013) 1329.
[67] L.I. Man, Kristallografiya 15 (1970) 471.
[68] I. Chaus, Yu.I. Gornikov, L.E. Demchenko, N.M. Kompanichenko, A.G. Grischuk, Russ. J. Inorg. Chem (Engl. Transl) 24 (1979) 346.
[69] Y. Ni, M. Shao, Z. Wu, F. Gao, X. Wei, Solid State Commun. 130 (2004) 297.